



Pharmaceutics, Drug Delivery and Pharmaceutical Technology

## Investigating Intra-Tablet Coating Uniformity With Spectral-Domain Optical Coherence Tomography



Yue Dong<sup>1</sup>, Hungyen Lin<sup>2</sup>, Vahid Abolghasemi<sup>3</sup>, Lu Gan<sup>4</sup>, J. Axel Zeitler<sup>5</sup>, Yao-Chun Shen<sup>1,\*</sup>

<sup>1</sup> Department of Electrical Engineering and Electronics, University of Liverpool, Brownlow Hill, Liverpool L69 3GJ, UK

<sup>2</sup> Department of Engineering, Lancaster University, Lancaster LA1 4YW, UK

<sup>3</sup> Faculty of Electrical Engineering, University of Shahrood, Shahrood 3619995161, Iran

<sup>4</sup> Department of Electronic and Computing Engineering, Brunel University, Uxbridge UB8 3PH, UK

<sup>5</sup> Department of Chemical Engineering and Biotechnology, University of Cambridge, Cambridge CB2 3RA, UK

### ARTICLE INFO

#### Article history:

Received 4 April 2016

Revised 19 September 2016

Accepted 21 September 2016

Available online 31 October 2016

#### Keywords:

coating  
optical coherence tomography  
imaging method  
process analytical technology  
tablet

### ABSTRACT

Spectral domain optical coherence tomography (SD-OCT) has recently attracted a lot of interest in the pharmaceutical industry as a fast and non-destructive modality for direct quantification of thin film coatings that cannot easily be resolved with other techniques. While previous studies with SD-OCT have estimated the intra-tablet coating uniformity, the estimates were based on limited number of B-scans. In order to obtain a more accurate estimate, a greater number of B-scans are required that can quickly lead to an overwhelming amount of data. To better manage the data so as to generate a more accurate representation of the intra-tablet coating uniformity without compromising on the achievable axial resolution and imaging depth, we comprehensively examine an algebraic reconstruction technique with OCT to significantly reduce the data required. Specifically, a set of coated pharmaceutical tablets with film coating thickness in the range of 60–100  $\mu\text{m}$  is investigated. Results obtained from performing the reconstruction reveal that only 30% of the acquired data are actually required leading to a faster convergence time and a generally good agreement with benchmark data against the intra-tablet coating uniformity measured with terahertz pulsed imaging technology.

© 2017 The Authors. Published by Elsevier Inc. on behalf of the American Pharmacists Association<sup>®</sup>. This is an open access article under the CC BY license (<http://creativecommons.org/licenses/by/4.0/>).

### Introduction

The process of coating one or more layers of polymer onto tablets is almost ubiquitous in pharmaceutical manufacturing in order to achieve uniformity of color, light protection, taste masking, and, more recently, advanced coatings such as active coatings and sustained release, where the drug release kinetics can be controlled thereby increasing the therapeutic efficacy of tablets.<sup>1</sup> In addition to average coating thickness, other benchmarks that govern the quality of the finished product include intra- and inter-tablet coating uniformity. Inter-tablet coating uniformity refers to the variations in coating thickness between different tablets within a batch, and a low level of variation is desired to ensure consistent quality across the batch. In contrast, intra-tablet uniformity

describes the variation in coating thickness on an individual tablet, and achieving a high level of intra-tablet uniformity is especially important in functional film coating, for instance, in sustained release formulations, where the drug release rate depends on the layer thickness of the film coating. To date, various measurement techniques have been employed for assessing the intra-tablet coating uniformity. These include laser-induced breakdown spectroscopy,<sup>2</sup> which is destructive in nature, and other non-destructive techniques such as hyperspectral near-infrared imaging,<sup>3,4</sup> ultraviolet (UV) chemical imaging,<sup>5</sup> X-ray micro-computed tomography,<sup>6</sup> terahertz pulsed imaging (TPI),<sup>7,8</sup> and, more recently, spectral-domain optical coherence tomography (SD-OCT).<sup>9–11</sup> However, near-infrared spectroscopy is inherently an indirect method as it needs additional reference techniques to build a calibration model. UV chemical imaging is able to map and differentiate the different types of coating defects<sup>5</sup> but it does not provide quantitative coating thickness information because of limited penetration depth of UV light into thick coatings. TPI and laser-induced breakdown spectroscopy can be used for quantifying

\* Correspondence to: Yao-Chun Shen (Telephone: +44 151 7944575; Fax: +44 151 7944540).

E-mail address: [y.c.shen@liverpool.ac.uk](mailto:y.c.shen@liverpool.ac.uk) (Y.-C. Shen).

thick coatings. Laser-induced breakdown spectroscopy requires high-energy laser pulses (100 mJ) which have relatively large spot size of 150  $\mu\text{m}$  diameter and low repetition rate of 10 Hz.<sup>2</sup> TPI can achieve higher data acquisition rate of hundreds of waveforms per second and high axial resolution of better than 40  $\mu\text{m}$ , but its lateral resolution is fundamentally limited by the relatively longer wavelength of THz radiation (300  $\mu\text{m}$  at 1 THz). On the other hand, X-ray micro-computed tomography provides micrometer resolution image of a tablet in all 3 dimensions but the data acquisition time is slow (1.8-3.5 h for each tablet<sup>6</sup>).

SD-OCT is thus fast gaining popularity as a non-destructive method for quantitative evaluation of pharmaceutical coatings because it offers both high data acquisition rate (27,800 waveforms per second<sup>12</sup>) and high spatial resolution (the lateral and axial resolutions are better than 10 and 5  $\mu\text{m}$ ,<sup>12</sup> respectively). While the previous studies with SD-OCT have been demonstrated to be able to estimate the intra-tablet coating uniformity, the estimates were based on limited number of B-scans such as 192 B-scans<sup>10</sup> and 100 B-scans<sup>13</sup> resulting in a limited area for the tablet's three-dimensional (3D) reconstruction. Understandably, the reason for this is because of the overwhelming size of the acquired dataset that can quickly become unmanageable. For example, for a tablet of diameter 8 mm, scanning it with an optical spot size of 10  $\mu\text{m}$  would generate a dataset greater than 1 GB. Algebraic reconstruction technique (ART)<sup>14,15</sup> with OCT, which is based on a similar concept to the recently developed compressive sensing technology,<sup>16,17</sup> was proposed very recently to significantly reduce data acquisition without compromising on axial resolution and imaging depth. In order to establish SD-OCT as a useful and practical modality for assessing the entire tablet surface, the number of measurement points should be kept down but still sufficient to provide an accurate representation of the intra-tablet coating uniformity. This article comprehensively examines the use of an ART-OCT to determine the optimal number of measurements required without loss of information.

## Materials and Methods

### Tablet Production

The samples used in this study comprise a batch of pharmaceutical tablets with a single sustained-release polymer coating layer. The tablet cores were biconvex shaped and contained 10% wt/wt

diprophyllin (API), 84.5% wt/wt lactose monohydrate (FlowLac<sup>®</sup> 100), 5% wt/wt vinylpyrrolidone-vinyl acetate copolymer (Kollidon<sup>®</sup> V64), and 0.5% wt/wt magnesium stearate. The transparent coating suspension has the following formulation: 50% wt/wt polyvinyl acetate (Kollicoat<sup>®</sup> SR 30D), 6% wt/wt polyvinyl alcohol-polyethyleneglycol graft copolymer (Kollicoat<sup>®</sup> IR), 0.075% wt/wt polyoxyethylene (20) sorbitan monooleate (Polysorbate 80), 0.3% wt/wt glycerolmonostearate, 0.75% wt/wt triethylcitrate, and 42.87% wt/wt deionized water. The tablet cores were coated in a pilot scale coater BFC25, Bohle Film Coater (L.B. Bohle, Ennigerloh, Germany). The coating pan dimensions were 546 mm in diameter and 630 mm in length and the batch size was 20 kg. The coater used 5 two-way spray nozzles (970/7-1 S75; Düsen-Schlick GmbH, Untersiemau, Germany) to spray coat the tablets. The geometry of a coated tablet is approximately 4 mm in height and 8 mm in diameter. A tablet was randomly selected after the following amounts of the sustained-release polymer were applied: 3.6, 5.5, 7.3, 9.1 mg/cm<sup>2</sup> on a pilot scale study.<sup>18</sup>

### Terahertz Pulsed Imaging Measurements

TPI measurements on the top and bottom surfaces of the tablets were performed using a TPI Imaga 2000 system (TeraView Ltd., Cambridge, UK). At each measurement point, the terahertz radiation reflected from a tablet sample was recorded as a function of time over a scan range of 2 mm. The TPI Imaga 2000 system is specifically developed for the fully automated scan of typical pharmaceutical solid dosage forms that usually have curved surfaces. A 6-axes robot system was employed to handle the tablets. This ensures that the tablet is always at the terahertz focus position with its surface perpendicular to the terahertz probe during a TPI measurement.<sup>8</sup> The terahertz radiation used here is broadband, covering a spectral range of 5-100 cm<sup>-1</sup> (0.15-3 THz). The spot size of the focused terahertz beam at the tablet surface is estimated to be about 200  $\mu\text{m}$  in diameter at its center frequency of 1.5 THz (50 cm<sup>-1</sup>). For the accurate determination of the coating layer thickness, the refractive index of the coating matrix is required. The refractive index of the coating was measured by terahertz time-domain spectroscopy using an uncoated tablet core as the reference. Using this method, a refractive index of 1.68-1.79 was determined<sup>18</sup> and a value of 1.74 was used for thickness quantification.

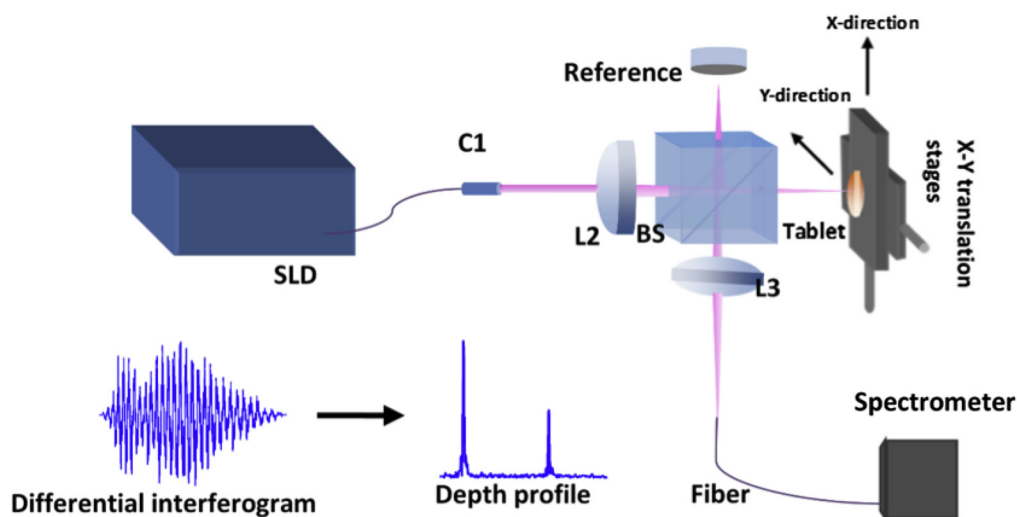


**Figure 1.** Schematic diagram of experimental setup. C1, collimator; L2 and L3, lenses; BS, 50:50 beam splitter; SLD, superluminescent diode. The insets are a typical differential interferogram and depth profile.

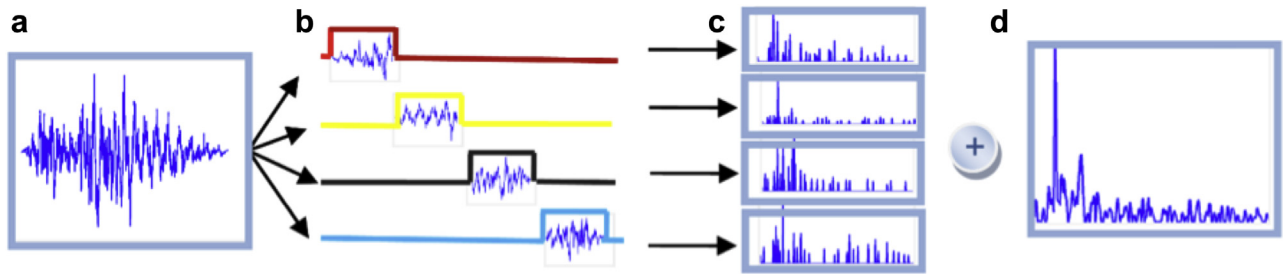


**Figure 2.** Flow chart of the spectrum split method combined with OMP algorithm. (a) Differential interferogram; (b) windowed differential interferogram; (c) sub-depth profiles, and (d) final depth profile.

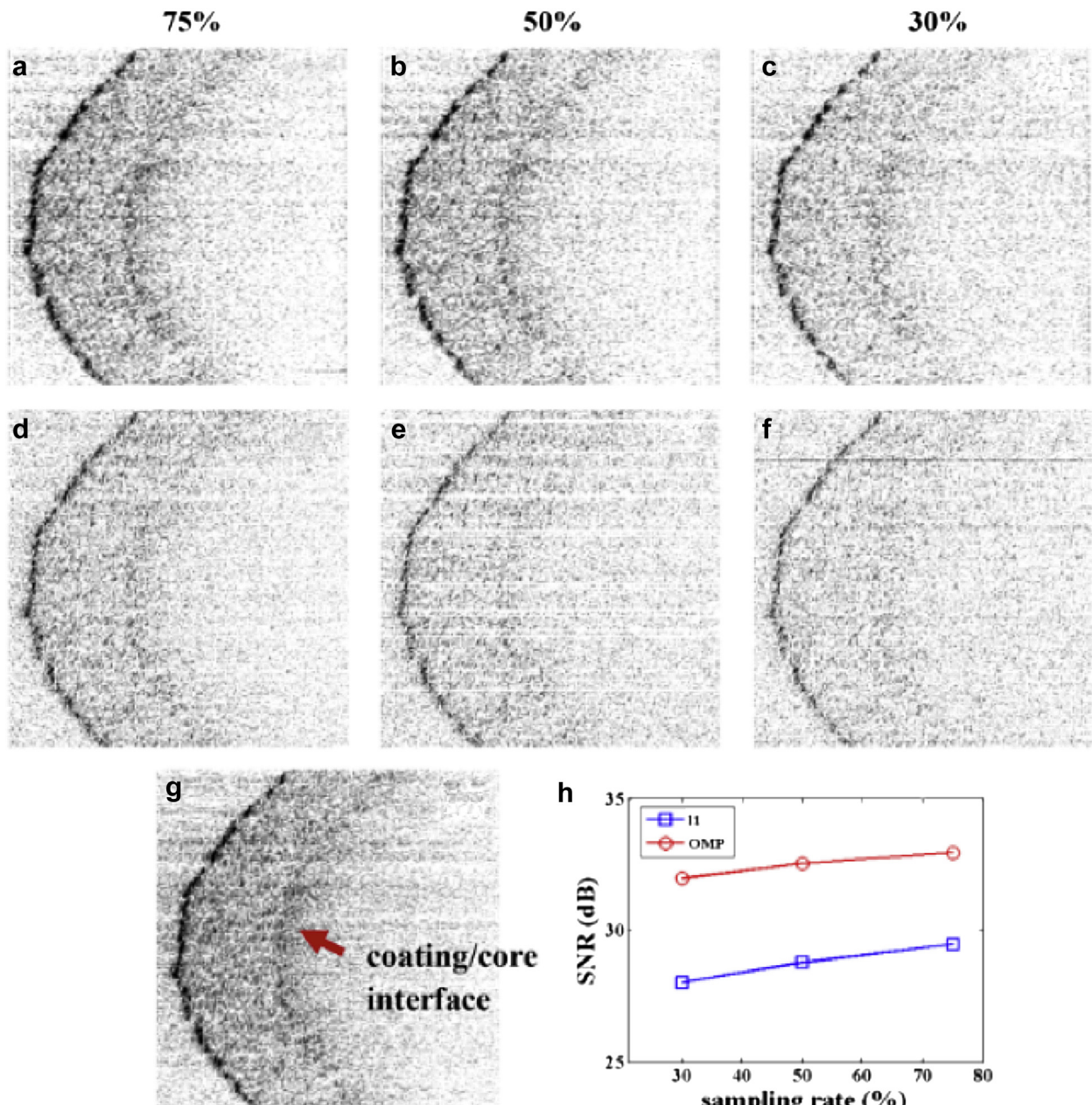


**Figure 3.** OMP reconstructed cross-sectional images of pharmaceutical tablet with a weight gain of 5.5 mg/cm<sup>2</sup>, using 75% (a), 50% (b), and 30% (c) random selected differential interferogram. L1 reconstructed cross-sectional images of the same tablet by using 75% (d), 50% (e), and 30% (f) random selected differential interferogram. (g) Conventional SD-OCT cross-sectional image. (h) SNR of each reconstructed images. Each of the reconstructed images contains 300 depth profiles and the image size is 3 × 0.3 mm<sup>2</sup>.

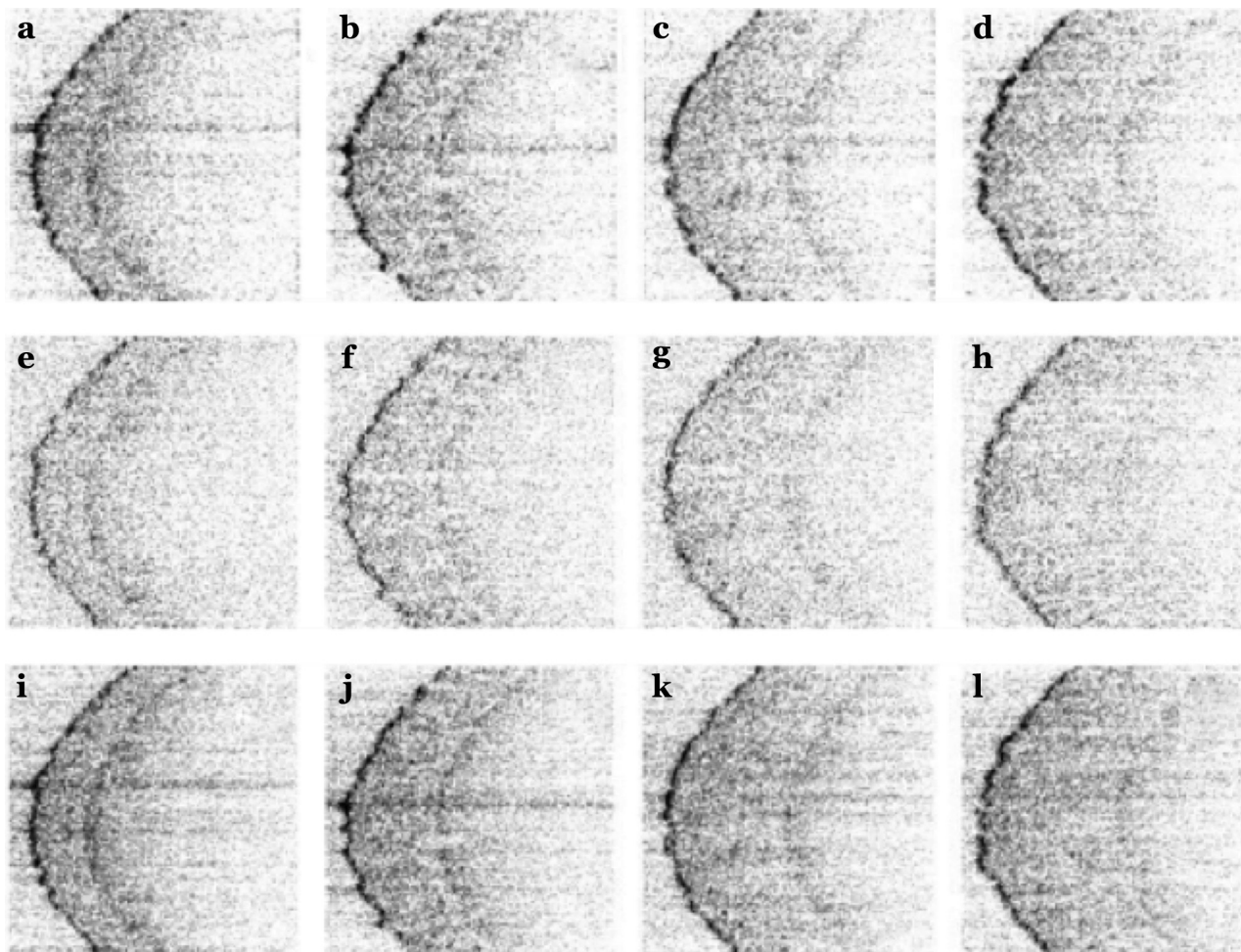


**Figure 4.** Cross-sectional images of tablet coating with a weight gain of 3.6, 7.3, 9.1, and 10.9 mg/cm<sup>2</sup>, reconstructed by (a-d) OMP combined with spectrum split method. (e-h) L1 optimization algorithm and (i)-(l) raw images. Each of the cross-sectional images contains 300 depth profiles and the image size is 3 × 0.3 mm<sup>2</sup>.

#### Spectral Domain Optical Coherence Tomographic Measurements

A conventional in-house SD-OCT system was used in the experimental measurements.<sup>11</sup> As shown in Figure 1, the light source used is a low coherence superluminescent diode EXS210040 (EXALOS, AG, Schlieren, Switzerland) operating at a center wavelength of 844 nm. The full width at half maximum of its spectral coverage is 132 nm. The collimated light beam was split into 2 arms by a 50:50 beam splitter, and focused onto the sample and a reference reflector by using a convex lens. The back reflected/scattered light from the reference reflector and the tablet were collected by another convex lens, recombined at the beam splitter, and finally delivered to a spectrometer using a multimode fiber. The spectrometer (Migtex) uses a line camera with 3648 pixels and has a spectral resolution of 0.5 nm.

In order to study the capability of the ART-OCT for reconstruction of OCT cross-sectional image (B-scans), 6 tablets with different coating thicknesses were measured. Each tablet was moved by a translation stage to acquire a single B-scan covering a length of 3 mm. At each measured pixel on the tablet surface, 2 interferograms (A-scans) were recorded with a phase shift of  $\pi$  which was introduced using a piezoelectric actuator. This phase shift method is advantageous in that the baseline and auto-correction terms will be automatically removed in the resultant differential spectral interferogram.

In order to measure the intra-tablet coating thickness uniformity of the whole tablet surface, 2 translation stages arranged perpendicular to each other were used to move the tablet sample. In total, 425 B-scans were acquired covering a tablet surface area of 10 mm × 8.5 mm and each B-scan consists of 1000 A-scans. The step size between successive A-scans and B-scans were 10 and 20  $\mu$ m, respectively. Due to such a large number of pixels (425,000), an alternative spectrometer (Cobra 800; Wasatch Photonics) with higher data acquisition speed (45,000 spectra per second) was used for 3D mapping. In addition, the spectrometer has higher spectral resolution (0.04 nm) but lower wavelength range (800-880 nm) that leads to lower axial resolution but higher imaging depth.

#### Reconstruction Method

In the ART-OCT method, the depth profile of a sample is directly reconstructed from the raw randomly sampled interferogram without the need of data interpolation that is required for conventional SD-OCT.<sup>14,15</sup> This is made possible because it relates the frequency measurements directly to the depth profile in an algebraic format like  $\mathbf{I} = \Phi \mathbf{R}$ , where  $\mathbf{I}$  denotes the interferogram in wavelength domain, vector  $\mathbf{R}$  is the sparse representation of the depth profile, and  $\Phi$  is the sensing matrix that also contains the spectral information of the light source used. Therefore by

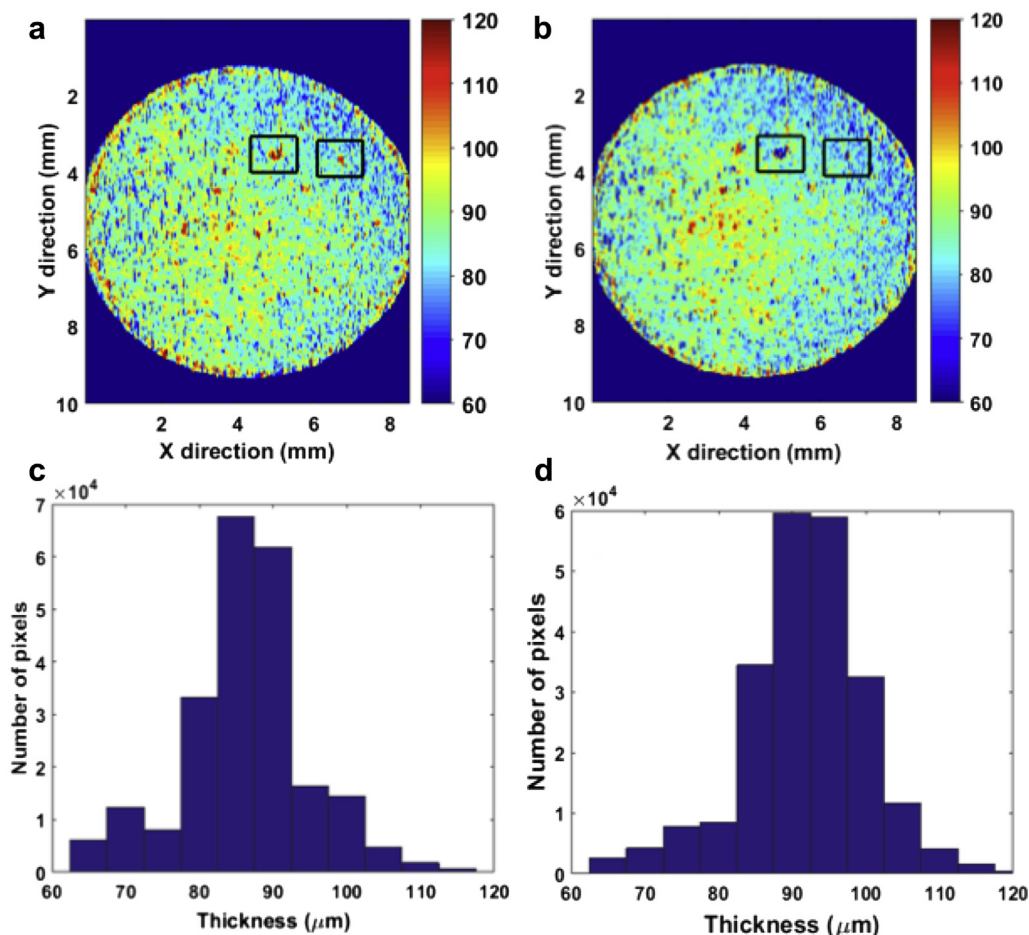


**Figure 5.** Spatial film coating thickness map of 5.5 mg/cm<sup>2</sup> sample generated by (a) 100% and (b) 30% measurement dataset and the respective thickness distribution generated by (c) 100% and (d) 30% measurement dataset. The square window identifies small artifacts introduced.

solving the algebraic inverse problem, the depth profile  $\mathbf{R}$  can be reconstructed from the compressed/resampled spectral interferogram data points. To speed up reconstruction, orthogonal matching pursuit (OMP)<sup>19</sup> is used together with the spectrum split approach instead of the L1 optimization algorithm proposed previously.<sup>14,15</sup>

#### OMP Reconstructed Depth Profile

The aim of the OMP algorithm is to select the column of the measurement matrix  $\Phi$  that correlates most with the residual  $\mathbf{r}$  of the interferogram (vector  $\mathbf{I}$ ) by greedy iterations.<sup>19</sup> The residual is defined as the difference between the original interferogram and its closest approximation at each iteration and it has an initial value corresponding to the resampled interferogram. In general, the problem of selecting the optimal column for the  $k$ th iteration can be formulated as

$$\varphi_k = \arg \max_{i=1,2,\dots,N} |\Phi_i^T \mathbf{r}_{k-1}| \quad (5)$$

where  $\varphi_k$  is the selected column index,  $\Phi_i^T$  is the transpose of the  $i$ th column in  $\Phi$ , and  $\mathbf{r}_{k-1}$  is the residual of interferogram calculated in the previous iteration. The index set  $\Gamma_k$  of non-zero elements is updated as follows:

$$\Gamma_k = \Gamma_{k-1} \cup \varphi_k \quad (6)$$

The current residual  $\mathbf{r}_k$  which will be used in the next iteration can be found as follows:

$$\mathbf{r}_k = \mathbf{I} - \Phi_{\Gamma_k} \Phi_{\Gamma_k}^+ \mathbf{I} \quad (7)$$

where  $\Phi_{\Gamma_k}$  stands for the selected subsets of matrix  $\Phi$ , and  $\Phi_{\Gamma_k}^+$  is its Moore-Penrose pseudo-inverse matrix.  $\Phi_{\Gamma_k} \Phi_{\Gamma_k}^+ \mathbf{I}$  is the closest approximation of the differential interferogram. The iteration will stop when all the indexes of non-zero elements in the depth profile are selected. At last the reconstructed depth profile is determined as follows:

$$\mathbf{R} = \Phi_{\Gamma}^+ \mathbf{I} \quad (8)$$

#### Spectrum Split Approach

Understandably, the interferograms of pharmaceutical film coatings contain many scattering features as a result of particle-like constituents where the number of scattering features varies from one dosage form to another.<sup>13</sup> Unfortunately, these features lead to the generation of pseudo-scattering features in the reconstructed depth profile when used in conjunction with OMP. To suppress the pseudo-scattering, we applied a spectrum split approach<sup>20</sup> to split up the spectral ranges by windowing as shown in Figure 2. The OMP reconstruction method was

**Table 1**  
Mean Thickness and Coefficient of Variation for Intra-Tablet Uniformity of Measured Tablets Obtained by 3D Reconstruction Using 100% and 30% Dataset

Weight Gain (mg/cm <sup>2</sup> )	Mean Thickness (μm)			CoV <sub>intra</sub>		
	100%	30%	TPI	100%	30%	TPI
3.6	61.1	64.8	67.7	0.105	0.118	0.103
5.5	79.5	84.3	83.7	0.097	0.096	0.149
7.3	101.4	103.3	101.2	0.074	0.080	0.179
9.1	121	118	120	0.048	0.064	0.1

subsequently applied on each of the split spectra. By doing so, real scattering features will remain while the pseudo-scattering features will be identified as they will appear at different depths that in turn can be removed by either averaging or subtraction. The number of split window is a trade-off between

the computational complexity and the suppress effect of pseudo-scattering.

## Results and Discussions

### Image Reconstruction

To demonstrate the efficacy of using the OMP algorithm in conjunction with the spectrum split approach, **Figures 3a-3c** show the cross-sectional images of the tablet that were reconstructed by using only 30%, 50%, and 75% of the randomly selected measurement data. As can be seen in **Figures 3a-3c**, the coating/core interface is clearly visible in all the reconstructed images with the proposed method. In contrast, the coating/core interface cannot be easily discriminated by the naked eye in images reconstructed with L1 optimization, as shown in **Figures 3d-3f**. To further quantify the

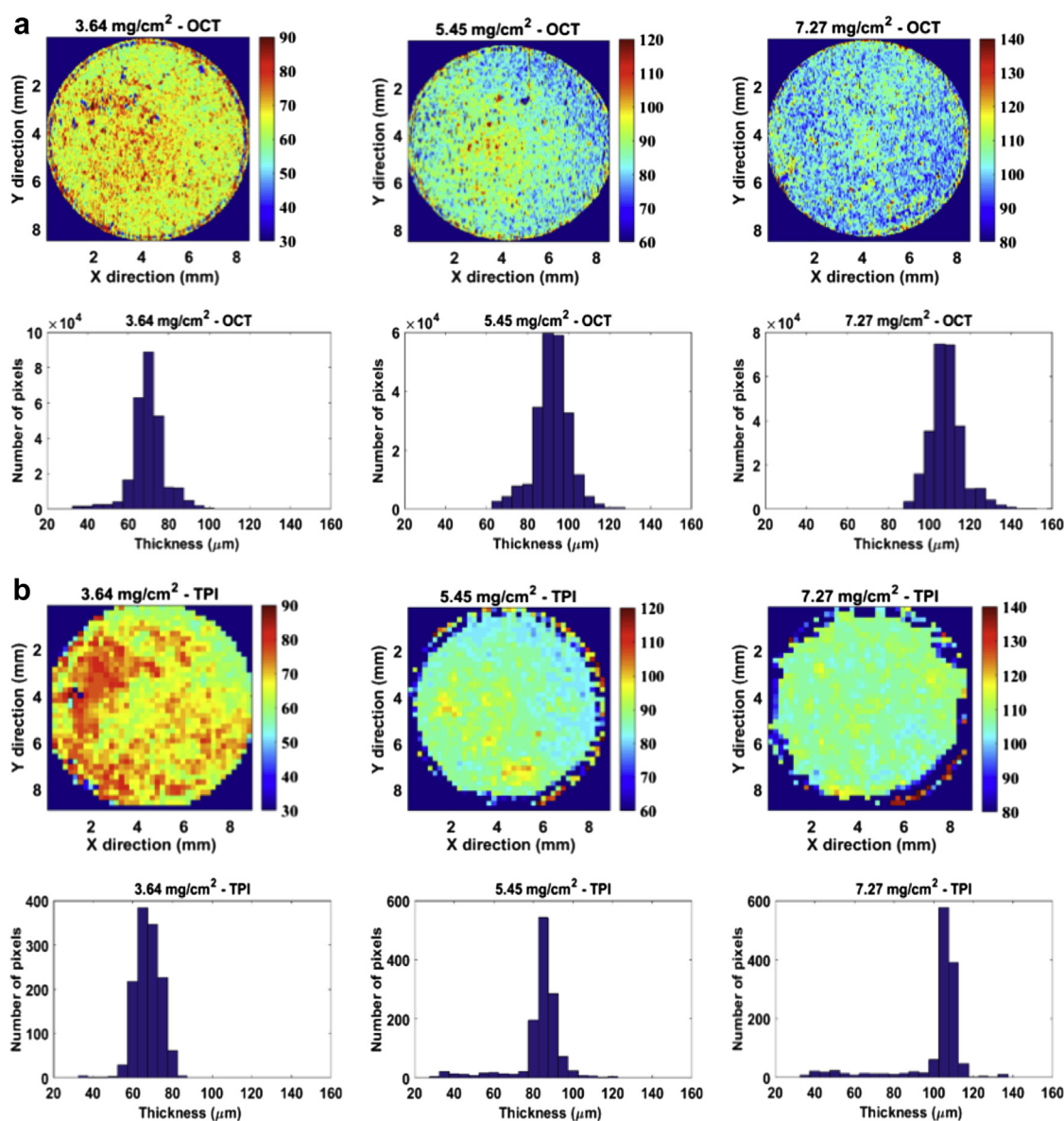


**Figure 6.** (a) OCT obtained thickness map and histogram distribution for tablets with a weight gain of 3.6, 5.5, and 7.3 mg/cm<sup>2</sup>. (b) TPI obtained thickness map and histogram distribution for tablets with a weight gain of 3.6, 5.5, and 7.3 mg/cm<sup>2</sup>.

reconstruction performance, the signal to noise ratio (SNR)<sup>16</sup> defined as

$$SNR = 10 \log_{10} \left( \frac{\max^2 I(x)}{\frac{1}{N} \sum (I(x) - i(x))^2} \right) \quad (9)$$

is used, where  $I(x)$  and  $i(x)$  are the intensities of the raw and reconstructed images, respectively. As shown in Figure 3h, our proposed method provides an improvement of 3.7 dB in SNR as compared with L1 optimization method.

In order to demonstrate the robustness of the proposed method for quantifying a range of coating thicknesses, we extend the analysis to all 5 tablets under investigation. With the reconstruction settings kept constant and a sampling rate of 75% to keep the highest possible imaging depth, the reconstructed cross-sectional images for the other tablets are shown in Figure 4. The coating/core interfaces in all the tablets are clearly visible in the cross-sectional images reconstructed by the proposed method as opposed to that reconstructed with L1 optimization method, where the coating/core interface becomes less visibly distinct with increased coating thickness.

#### Reconstruction Validation

With the ability to robustly reconstruct the cross-sectional images, the entire tablet can effectively be reconstructed by using only 30% of the acquired dataset. In order to generate a film coating thickness map so as to resolve spatial film thickness distribution, the mean depth profile of neighboring  $3 \times 3$  individual depth profiles was generated. The mean depth profile of the region of interest is subsequently used to calculate the coating thickness as the distance between the surface and the coating/core interface. In principle, other automated thickness calculation techniques such as these based on peak finding<sup>13</sup> and image segmentation methods<sup>21</sup> could also be applied. As an example, Figures 5a and 5b compare the spatial film coating thickness distribution for the tablet with  $5.5 \text{ mg/cm}^2$  weight gain generated with 100% and 30% of the dataset, respectively. Apart from a few minor artifacts as highlighted in the square windows, there is generally a good match between the 2 coating thickness maps. Figures 5c and 5d further compare the respective thickness histogram distribution taking account of the refractive index of the coating material in the near-infrared spectral range as previously determined.<sup>13</sup> Again, there is generally a good agreement between the coating distribution obtained by 100% and 30% dataset. The intra-tablet coating uniformity can also be quantified as the ratio of the standard deviation of the film coating thickness over the mean film thickness across the tablet's surface ( $\text{CoV} = \sigma/\mu$ ).<sup>22</sup> Table 1 compares the mean thickness and coefficient of variation for coating thickness maps reconstructed using 30% and 100% dataset. It is evident that there is no significant loss of information using only 30% of dataset in image reconstruction.

#### Intra-Tablet Coating Uniformity

As a further validation, Figure 6 compares the film coating thickness maps measured with the proposed ART-OCT method and that obtained by using the more established TPI method. Note that only the tablets with 3.6, 5.5, and  $7.3 \text{ mg/cm}^2$  weight gain were compared in this instance as coating thickness greater than  $100 \mu\text{m}$  has previously been found to produce unreliable results.<sup>13</sup> In general, the reconstructed SD-OCT thickness maps show a good qualitative agreement with the TPI thickness maps. Evidently, SD-OCT is advantageous over TPI in terms of the

achievable spatial resolution and data acquisition rate, which is at least 2 orders of magnitude higher than TPI. With this significant increase in the measurement data points, OCT provides more accurate representation of the intra-tablet coating uniformity. The thickness distributions from the respective techniques and Table 1 further show a good quantitative agreement. However, it should be highlighted that OCT measurement was not performed perpendicular to the curvature of tablet resulting in a worst case error of 11% at the tablet edge from the tablet center. This error can be mitigated either in hardware means such as a robotic arm in TPI<sup>8</sup> or compensated by post-processing code that has been developed for in-line monitoring of pellet coating.<sup>23</sup> In addition, because of the surface and coating/core interface in OCT B-scan images were picked up in specific area of interest, OCT generated a narrower thickness distribution than TPI contrary to expectation.<sup>13</sup>

#### Conclusion

SD-OCT is emerging as a suitable modality for the non-destructive evaluation of pharmaceutical coatings. It has a high data acquisition rate of over 20,000 waveforms per second and a high spatial resolution of better than  $10 \mu\text{m}$ . This allows the entire tablet to be scanned with high resolution providing a more accurate assessment of intra-tablet coating uniformity. One of the challenges is to efficiently deal with data acquisition and data processing of the large OCT dataset. In this article, we proposed a fast sparse optimization algorithm OMP in conjunction with the spectrum split approach to reconstruct depth profiles of pharmaceutical tablets. We found that using the proposed method, only 30% of the acquired dataset is necessary in order to reconstruct the depth profiles of the whole tablet. The proposed method was also found to be applicable to a range of film coating thicknesses. The work is relevant as it seeks to combat the challenge of being overwhelmed with too much data, while addressing the issue of generating a more accurate estimate of the intra-tablet coating uniformity by comparison against the more established TPI.

#### Acknowledgments

The authors would like to acknowledge the financial support from UK EPSRC Research Grant EP/L019787/1 and EP/L019922/1. H.L. also acknowledges travel support from Joy Welch Educational Charitable Trust.

#### References

- McGinity JW, Felton LA. *Aqueous Polymeric Coatings for Pharmaceutical Dosage Forms*. 3rd ed. London: Informa Healthcare; 2008.
- Madamba MC, Mullett WM, Debnath S, Kwong E. Characterization of tablet film coatings using a laser-induced breakdown spectroscopic technique. *AAPS Pharm Sci Tech*. 2007;8(4):184-190.
- Cairós C, Amigo JM, Watt R, Coello J, Maspoch S. Implementation of enhanced correlation maps in near infrared chemical images: application in pharmaceutical research. *Talanta*. 2009;79(3):657-664.
- Palou A, Cruz J, Blanco M, Tomás J, De Los Ríos J, Alcalá M. Determination of drug, excipients and coating distribution in pharmaceutical tablets using Nir-Ci. *J Pharm Anal*. 2012;2(2):90-97.
- Klukkert M, Wu JX, Rantanen J, et al. Rapid assessment of tablet film coating quality by Multispectral UV imaging. *AAPS PharmSciTech*. 2016;17:958-967.
- Russe IS, Brock D, Knop K, Kleinebudde P, Zeitler JA. Validation of terahertz coating thickness measurements using X-ray microtomography. *Mol Pharm*. 2012;9(12):3551-3559.
- Fitzgerald AJ, Cole BE, Taday PF. Nondestructive analysis of tablet coating thicknesses using terahertz pulsed imaging. *J Pharm Sci*. 2005;94:177-183.
- Zeitler JA, Shen Y, Baker C, Taday PF, Pepper M, Rades T. Analysis of coating structures and interfaces in solid oral dosage forms by three dimensional terahertz pulsed imaging. *J Pharm Sci*. 2007;96:330-340.

9. Mauritz JM, Morrisby RS, Hutton RS, Legge CH, Kaminski CF. Imaging pharmaceutical tablets with optical coherence tomography. *J Pharm Sci.* 2010;99:385-391.
10. Koller DM, Hanneschläger G, Leitner M, Khinast JG. Non-destructive analysis of tablet coatings with optical coherence tomography. *Eur J Pharm Sci.* 2011;44:142-148.
11. Zhong S, Shen YC, Ho L, et al. Non-destructive quantification of pharmaceutical tablet coatings using terahertz pulsed imaging and optical coherence tomography. *Opt Lasers Eng.* 2011;49:361-365.
12. Markl D, Hanneschläger G, Sacher S, Leitner M, Khinast JG. Optical coherence tomography as a novel tool for in-line monitoring of a pharmaceutical film-coating process. *Eur J Pharm Sci.* 2014;55:58-67.
13. Lin H, Dong Y, Shen YC, Zeitler JA. Quantifying pharmaceutical film coating with optical coherence tomography and terahertz pulsed imaging: an evaluation. *J Pharm Sci.* 2015;104:3377-3385.
14. Leitgeb R, Hitzinger CK, Fercher AF. Phase shifting algorithm to achieve high speed long depth range probing by frequency domain optical coherence tomography. *Opt Lett.* 2000;28:2201-2203.
15. Seck HL, Zhang Y, Soh YC. Optical coherence tomography by using frequency measurements in wavelength domain. *Opt Express.* 2011;19:1324-1334.
16. Liu XA, Kang JU. Compressive SD-OCT: the application of compressive sensing in spectral domain optical coherence tomography. *Opt Express.* 2010;18:22010-22019.
17. Liu CY, Wang A, Bizheva K, Fieguth P, Bie HX. Homotopic, non-local sparse reconstruction of optical coherence tomography imagery. *Opt Express.* 2012;20:10200-10211.
18. Ho L, Muller R, Gordon KC, et al. Terahertz pulsed imaging as an analytical tool for sustained-release tablet film coating. *Eur J Pharm Biopharm.* 2009;71:117-123.
19. Tropp JA, Gilbert AC. Signal recovery from random measurements via orthogonal matching pursuit. *IEEE Trans Inf Theor.* 2007;53:4655-4666.
20. Jia YL, Tan O, Tokayer J, et al. Split-spectrum amplitude-decorrelation angiography with optical coherence tomography. *Opt Express.* 2012;20:4710-4725.
21. Markl D, Sacher S, Leitner M, Khinast JG, Buchsbaum A. Automated pharmaceutical tablet coating layer evaluation of optical coherence tomography images. *Meas Sci Technol.* 2015;26:035701.
22. Freireich B, Wassgren C. Intra-particle coating variability: analysis and Monte-Carlo simulations. *Chem Eng Sci.* 2010;65(3):1117-1124.
23. Markl D, Zettl M, Hanneschläger G, et al. Calibration-free in-line monitoring of pellet coating processes via optical coherence tomography. *Chem Eng Sci.* 2015;125:200-208.